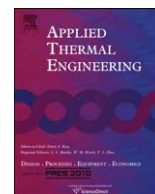




Contents lists available at SciVerse ScienceDirect

Applied Thermal Engineering

journal homepage: www.elsevier.com/locate/apthermeng

A study on a ventilation stack integrated with a light pipe

Q1 Thanyalak Taengchum^a, Surapong Chirarattananon^{a,b,*}, Robert H.B. Exell^{a,b}, Kuskana Kubaha^c, Pipat Chaiwiwatworakul^{a,b}^aJoint Graduate School of Energy and Environment, King Mongkut's University of Technology Thonburi, Bangkok, Thailand^bScience and Technology Postgraduate Education and Research Development Office, Ministry of Education, Thailand^cSchool of Energy Environment and Materials, King Mongkut's University of Technology Thonburi, Bangkok, Thailand

H I G H L I G H T S

- An experimental and theoretical study of solar heated stack-light pipe is reported.
- Solar heated water exchanges heat with air to create a stack flow.
- Wind, stack, and heat transfer effects are simultaneously coupled.
- The volume of air flow is sufficient for ventilation and passive cooling.
- The light pipe transmits sufficient natural daylight for general illumination.

A R T I C L E I N F O

Article history:

Received 11 November 2011

Accepted 19 April 2012

Available online xxx

Keywords:

Natural ventilation

Daylighting

Thermal buoyancy

Light pipe

Counter flow heat exchanger

Solar water heater

A B S T R A C T

A theoretical and experimental study has been conducted on the performance of a vertical light pipe that also functions as an air flow stack for night ventilation. The rectangular light pipe of height 3 m and cross-section area 0.0625 m² surrounded by an air duct of total cross-section area 0.23 m² is situated above a room of height 3.8 m and floor area 9 m². Heat transfer from the hot water in the wraparound hot water jacket to the air in the duct is assisted by stainless steel fins. The ventilation of the room, due partly to the buoyancy of the air in the duct and partly to the wind effect, amounted to nearly 10 air changes per hour which is sufficient for passive cooling during cooler night periods. The light pipe has specular reflecting walls. It was found that the transmission of daylight through the light pipe in the middle of a partly cloudy day was sufficient for illuminating the room to general illumination level.

© 2012 Published by Elsevier Ltd.

1. Introduction

The climate of Thailand is hot and humid. Air-conditioning to provide cooling for thermal comfort has been increasingly used in consonant with the increase in disposable income. Air-conditioning load accounts for over 70% of total electric load in a small household. However, night time air is cool and it is possible to use natural ventilation to achieve thermal comfort in detached houses in suburban areas for most nights of a year.

A report of the National Statistical Office of Thailand on the appliance ownership in Thailand, [1], shows that 14.3% and 12.8% of all households own air-conditioners and electric hot water heaters

(used for personal hygiene-bathing) in 2008. Among all households, more than 40% of middle and high income households own both air-conditioners and electric hot water heaters. It seems that ownerships of air-conditioners and electric hot water heaters correlate strongly and both are increasing steeply. The authors perceive that warm water (at 40–50 °C) produced by heat pump air-conditioner while running as room air-conditioner, or by solar hot water heater, could be used to produce and store warm water to drive stack air flow for night ventilation. In the latter case, cooling and ventilation are completely passive.

The device in this paper integrates a light pipe and a ventilation stack in the same unit that will reduce construction cost. The whole unit is expected to be situated in a large space at the middle of a house. Daylight transmitted through the light pipe will provide general lighting for the space during daytime while stack air flow will provide night ventilation. In this paper, raytracing is used for calculation of both daylight from sun and that from sky. A well-known sky luminance distribution model is used with measured

* Corresponding author. Joint Graduate School of Energy and Environment, King Mongkut's University of Technology Thonburi, Bangkok, Thailand. Tel.: +66 (2) 4708309.

E-mail addresses: t.thanyalak@yahoo.com (T. Taengchum), surapong@jgsee.kmutt.ac.th (S. Chirarattananon), exell@jgsee.kmutt.ac.th (R.H.B. Exell), kuskana.kub@kmutt.ac.th (K. Kubaha), pipat_ch@jgsee.kmutt.ac.th (P. Chaiwiwatworakul).

Nomenclature¹

ΔP_{stack}	stack pressure at the stack inlet or outlet
g	constant of gravity, 9.81
ρ_a	density of air at inlet
h_s	stack height
h_{NL}	neutral height
T_s	temperature of air at stack outlet
T_a	temperature of air at stack inlet
\dot{V}_{sin}	rate of volumetric flow of air at stack inlet
\dot{V}_{sout}	rate of volumetric flow of air at stack outlet
A_s	cross-sectional area of stack
C_{Di}	discharge coefficient of air flow through an opening
ΔP_{sin}	stack pressure inlet
ΔP_{sout}	stack pressure outlet
ns	exponent of stack pressure
P_{wi}	wind pressure at wall i
C_{pi}	local pressure coefficient at wall i
v_i	speed of wind into wall i

\dot{V}_{wi}	rate of volumetric flow of air due to wind at wall i
A_{wi}	area of wall i
nw	exponent of wind pressure
d_p	internal counter balancing pressure against wind pressure
ε	effectiveness of (stack) heat exchanger
N	number of transfer units
M_a	heat capacity flow rate of air
M_w	heat capacity flow rate of water
R	ratio of heat capacity flow rate
U	overall heat transfer coefficient
UA_a	air-side heat transfer parameter
ΔT	log mean temperature difference (LMTD)
ρ_s	density of air at stack outlet
P_f	pressure loss due to friction
f	friction factor
D_h	hydraulic diameter
C_{ps}	wind pressure coefficient at stack outlet

daylight illuminance data obtained from a nearby station on the same campus. A heat exchange model is integrated with a stack air flow model to predict the rate of air flow in the stack. However, the actual air flow is disturbed by wind and the model is modified to account for the effect of wind. The integrated model is used to calculate air flow under the situation of the experiment.

Zhai and Previtali, [2], in a review of vernacular architecture, identify local climate and cultural heritage as the main influences on ancient architecture of a location. The authors use vernacular houses in two locations in Indonesia where the houses are constructed on raised floor with open windows and doors for natural ventilation for illustration. Natural ventilation and daylighting are two methods that can help reduce energy needs in modern buildings. Normally, they are separate and independent operations. However, in a project supported by the European Union and participated by five European institutions in five countries called 'TripleSave', [3], it was demonstrated that a light pipe can be integrated with a ventilation stack and used with passive or active heating or cooling system to serve three functions of daylighting, ventilation, and heating or cooling of buildings. A number of publications by participating institutions illustrate theoretically and experimentally the effectiveness of light transmission of light pipes fitted with different light entry ports and surface material, [4–6], and the effectiveness of air flow through different ventilation terminals that are subjected to wind from different directions, [7,8]. Air flow by natural means is due to pressure differences caused by wind and thermal buoyancy. In the case of buoyancy air flow in a solar chimney, a number of studies have been reported, such as those in Refs. [9–11], where heat transfer from solar radiation to air creates buoyancy force to drive air flow through stack, [12,13]. Studies of wind effect on air flow into buildings have also been conducted, [14–16]. The methods used in Refs. [9–16] have not been directly applied to the case of simultaneous heat transfer to air in a stack when the air flow is subjected to the influence of wind at the stack outlet. Superposition method with simplified model has been employed for the mixed wind and stack driven flow in some studies, [17,18]. However, computational fluid dynamics (CFD) instead has been reportedly used to study stack air flow that is simultaneously subjected to the force of wind, [19], and also to solar heating, [20].

Light pipes are hollow light guidance systems with highly reflective interior surfaces that are used to transfer natural daylight from both the sun and the sky from the exterior of a building into its interior spaces. Light pipes comprising circular cross sections (or cylindrical shape) are more commonly used than those comprising rectangular cross sections. Raytracing and flux transfer have been applied successfully to the study of façade-mounted rectangular pipes by Hien and Chirarattananon, [21]. Dutton and Shao, [22], use long thin rectangular sections to form approximate circular shaped pipes and simulate light pipe transmission by the use of Photopia, a computer program. Swift et al., [23], develop theoretical model of transmission of rectangular light pipe for collimated rays and report that results from the model agree well with experimental results.

2. Thermal environment and vernacular architecture

Traditional practice of housing construction is influenced by and reflects the climate of the location and cultural heritage, [2]. Prior to the advent of air-conditioning, buildings in Thailand were designed for natural ventilation.

Dry-bulb temperature of the central region of Thailand varies from 25° to 35 °C over a daily range of about 10 °C for every day except those in the cooler period of November to January. Daily range of relative humidity is 40–80%. For most nights, air temperature in suburban and less densely populated area surrounding a detached house is sufficiently cool for night ventilation. Table 1 shows the percentage number of hours in a year between 10 PM and 7 AM that ambient temperature falls below the given value. Among the middle income people who own air-conditioners, the present practice is to turn the air-conditioners in the bedrooms on to sleep at night. The configuration of the stack proposed in this paper will enable utilization of cool natural air for ventilation for the same purpose.

Table 1

Number of hours between 10 PM and 7 AM in a year that the ambient temperature falls within the given value.

Temperature, °C	30	29	28	27	26	25
Number of hours	3286	3256	3095	2664	1925	1099
% of number of hours between 10 PM and 7 AM	100	99	94	81	59	33

¹ Listed in order of appearance.

Fig. 1 shows monthly average hourly temperatures. Hourly temperatures of the four months of November to February exhibit distinct pattern of the cooler season where the values are lower than those of all other months during the night to the early morning period. If the acceptable temperature is 27 °C, the air is sufficiently cool for over 80% of the night time period in a year, as seen from Table 1.

3. Experimental set up

The configuration of the light pipe and solar-heated ventilation stack is shown in Fig. 2, and a cross-section of the stack interior, which has five concentric layers, is shown in Fig. 3. The fins, which transfer heat from the water to the air in the duct, are of stainless steel 1.2 mm thick. The volume of hot water to be contained by the jacket is 0.286 m³. The insulation layers are of fiberglass 12.5 mm thick.

Fig. 4 shows a vertical side view of the stack, which is 3 m high and is situated above the ceiling of the experimental room. Thermally insulated half-inch copper pipes were used between the solar water heater tank and the stack water jacket. Hot water from the solar collector tank was pumped downwards through the water jacket causing the air inside the stack to rise in counter flow. The stack water jacket and the air duct act as a counter flow heat exchanger. Typical values of thermal conductivities of copper and stainless steel are used for calculation of heat transfer parameters. The water side heat transfer area is 6.6 m² while that for the air side is 22.5 m². The estimated value of the overall heat transfer parameter (UA value) is 56 W K⁻¹.

The light pipe transmits daylight to the interior space, which has four doors, as shown in Fig. 5. A chamber of 1.1 m height at the top of the stack has downward-pointing black-painted slats to allow air to escape and keep out rain. The glass cover at the top of the pipe has transmittance 88%. The walls of the light pipe are covered with specularly reflecting plastic film having reflectance 99%. The bottom of the light pipe is covered with a translucent plastic plate used to diffuse the light.

The size of the light pipe was chosen so that there was sufficient light flux to illuminate the room. The size of air duct was chosen to allow sufficient air flow for ventilation. The height of the stack of 3.0 m was determined to create sufficient stack pressure and flow.

A daylight measurement station has been set up on top of a nearby 7-storey building on the seaside campus of the university. Beam normal illuminance and irradiance are measured directly by a suntracker. The tracker also holds two shading balls to shade out sunlight and sun irradiance from an illuminance sensor and an

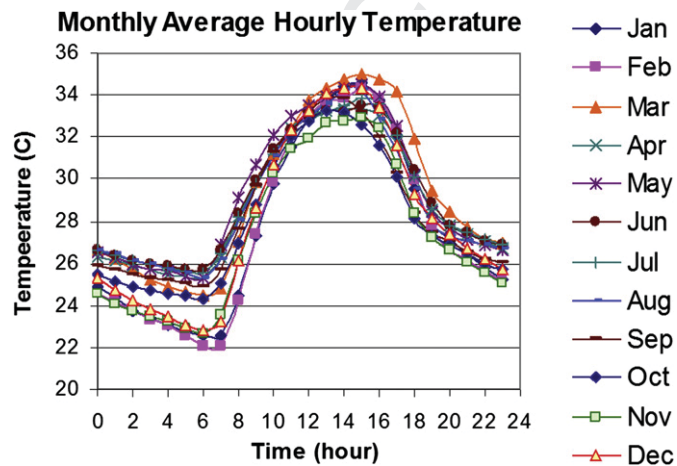


Fig. 1. Monthly average hourly temperature.



Fig. 2. Light pipe and solar heated ventilation stack.

irradiance sensor to give values of diffuse sky illuminance and diffuse irradiance. Global illuminance and global irradiance as well as total illuminance and total irradiance in each cardinal direction are measured by individual sensors. Measured data of sun and sky illuminance from the station were used in the calculation described in the followings.

4. Mathematical models

The stack with hot water that flows through its jacket performs as a water to air heat exchanger. The heated air flows up through the stack by buoyancy force. The room where the stack is situated has four openings (door and windows) that are subjected to the force of wind. The mechanisms of heat transfer and air flows in the three connected components can be described by three coupled mathematical models as follows.

4.1. Air flow through stack

The pressure difference that drives airflow through a stack due to buoyancy force can be determined by the following relationship, [12,13],

$$\Delta P_{\text{stack}} = \frac{g\rho_a(h_s - h_{\text{NL}})(T_s - T_a)}{T_s} \quad (1)$$

where ΔP_{stack} is the pressure difference at the stack inlet (when $h_s = 0$) or the stack outlet (when $h_s = \text{stack height}$), g is the gravity constant, ρ_a is the density of air at the inlet, h_{NL} is the neutral height,

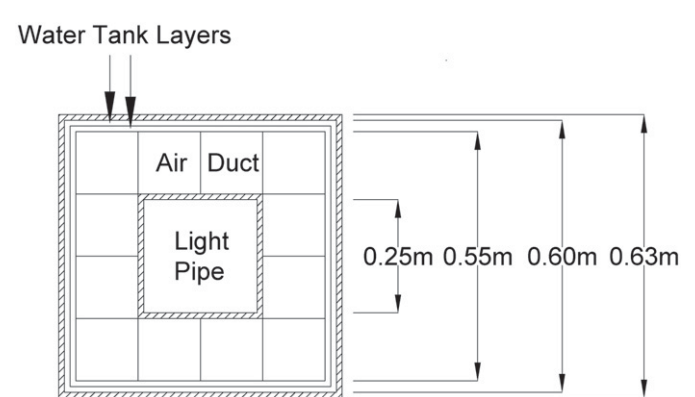


Fig. 3. Horizontal cross-section of stack. Air duct is divided into 12 square channels by stainless steel fins. Layers of thermal insulation are shaded.

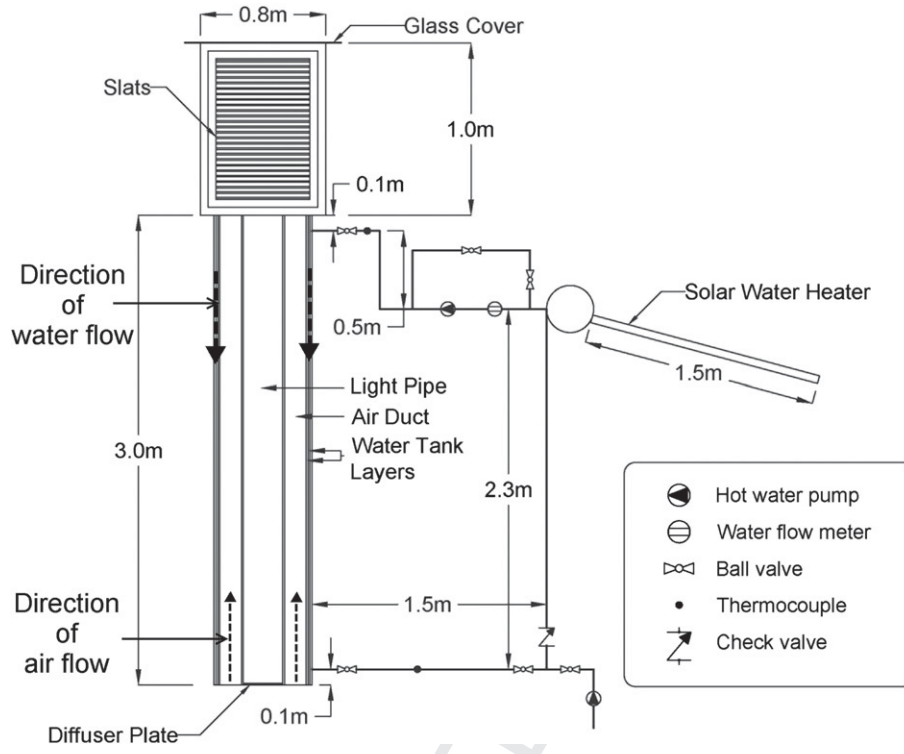


Fig. 4. The three system components.

T_s is the temperature of the air at the stack outlet, and T_a is the temperature of the air at the stack inlet.

The neutral height h_{NL} is an unknown. For a simple stack where the stack dimension and air temperatures are known, equation of balance of air flows can be set up from which the neutral height can be obtained.

The volumetric rates of air flow \dot{V}_{sin} into and \dot{V}_{sout} out of the stack are determined by

$$\dot{V}_{sin} = A_s C_{Di} \frac{\Delta P_{sin}}{|\Delta P_{sin}|^{1-ns}} \quad \text{and} \quad \dot{V}_{sout} = A_s C_{Di} \frac{\Delta P_{sout}}{|\Delta P_{sout}|^{1-ns}} \quad (2)$$

where A_s is the cross-sectional area of the stack, C_{Di} is a discharge coefficient, and ns is an exponent. In this research the inlet area equals the outlet area.

4.2. Air flow due to wind

When wind is present, the wind pressure on each external facade of a room superimposes a pressure to the air at a given location. The pressure difference P_{wi} between the wind pressure on the wall i and the (static) local outdoor air pressure at the same location is given by Ref. [16] as

$$P_{wi} = \frac{1}{2} C_{pi} \rho_a v_i^2 \quad (3)$$

where C_{pi} is a local pressure coefficient the value of which is dependent on the direction of the wind on the facade, and v_i is the wind speed. References [14,15] give average value of local wind pressure coefficient on a wall in a given direction.

The volume flow rate \dot{V}_{wi} of air into the room through an opening of area A_{wi} in the wall is given by the formula, [16],

$$\dot{V}_{wi} = A_{wi} C_{Di} P_{wi}^{nw} = \frac{A_{wi} C_{Di} P_{wi}}{|P_{wi}|^{1-nw}} \quad (4)$$

where C_{Di} is a discharge coefficient, and nw is an exponent between 0.4 for large openings and 1.0 for small openings. The second equality in Equation (4) is used to preserve the sign of the volumetric flow \dot{V}_{wi} which can be negative. In a contiguous room with openings, the sum of air flows into the room must balance to zero for all wind velocity and for any room configuration. This implies that there is a counter-balancing pressure from the interior of the room to enable the flows of air into and out of the room to balance out. Let this counter balancing pressure in the room in Fig. 5 be d_p . Then for opening i , the net wind pressure on the opening is given as

$$P_{wi} = \frac{1}{2} C_{pi} \rho_a v_i^2 - d_p \quad (5)$$

4.3. Heat transfer in the stack

The temperature of the air entering the stack at the bottom is assumed to be the ambient air temperature T_a in the room. Let T_{wi} be the temperature of the water flowing into the top of the water jacket around the stack from the solar water tank. Then the temperature T_s , which is the temperature that air emerges from the stack is raised to, is given by Ref. [24] as

$$T_s = T_a + \varepsilon(T_{wi} - T_a) \quad (6)$$

where ε is the effectiveness of the heat exchange process in the stack. This value is obtained from

$$\varepsilon = \frac{1 - \exp[-N(1 - R)]}{1 - R \exp[-N(1 - R)]} \quad (7)$$

where N is the number of heat transfer units, and R is ratio of the heat capacity flow rates of air M_a and water M_w . The quantity N is related to heat capacity flow rates and the heat exchanger

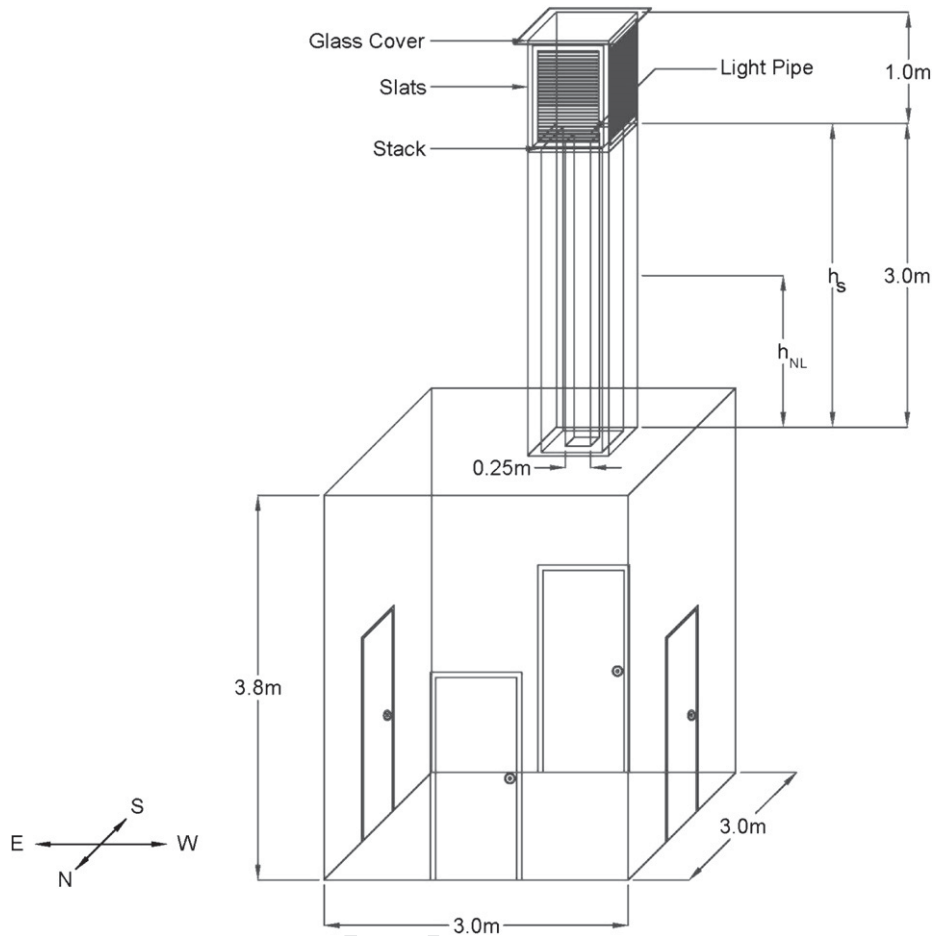


Fig. 5. The experimental room and stack (sloping roof not shown).

parameter UA_a , where U is the overall heat transfer coefficient and A_a is the heat transfer area (air-side) of the heat exchanger. The value of UA_a (The same UA value as that in Section 3) is related to the heat transfer rate Q by the equation,

$$Q = UA_a \Delta T, \quad (8)$$

where ΔT is the log mean temperature difference (LMTD) across the heat exchanger, see Ref. [21]. In Equation (6), T_s (and T_{wo} as well) is dependent on ϵ , which is in turn dependent on the rate of heat capacity flow of air, M_a or the volumetric flow rate of air through the stack, \dot{V}_{sin} or \dot{V}_{sout} in Equation (2).

4.4. Combined equations

When wind exerts pressure onto the experimental room with the stack-light pipe in Fig. 5, air can flow through all four openings and through the outlet on top of the stack. The mass balance equation for air flowing through the room is written as

$$\left[\sum_{i=1-4} \rho_a \dot{V}_{wi} \right] + \rho_s \dot{V}_{sout} = 0, \quad \text{or} \quad \left[\sum_{i=1-4} \rho_a A_{wi} C_{Di} \frac{\frac{1}{2} C_{pi} \rho_a v_i^2 - d_p}{\frac{1}{2} C_{pi} \rho_a v_i^2 - d_p} \right] + \rho_s \dot{V}_{sout} = 0 \quad (9)$$

where ρ_{out} is the density of air at the outlet of the stack. The counterbalancing pressure d_p for this experimental room also exerts on the inlet (bottom) of the stack, thus modifying the pressure at the inlet. The wind pressure also exerts at the top of the stack, thus modifying the pressure at the stack outlet. The roughness of the interior surface of the stack can act to reduce the flow of air through the stack. The pressure loss due to this friction force is given by the Darcy–Weisbach equation, [21], as

$$P_f = f \frac{h}{D_h} \rho_a \frac{v_{in}^2}{2}$$

where f is the friction factor and D_h is the hydraulic diameter. The resultant mass balance equation at the stack then becomes

$$\rho_a \dot{V}_{sin} + \rho_s \dot{V}_{sout} = 0, \quad \text{or} \quad \frac{\rho_a \Delta P_{sin}}{|\Delta P_{sin}|^{1-ns}} + \frac{\rho_s \Delta P_{sout}}{|\Delta P_{sout}|^{1-ns}} = 0 \quad (10)$$

where, $\Delta P_{sin} = -(g\rho_a(-h_{NL})(T_s - T_a)/T_s) + d_p - P_f$ and $\Delta P_{sout} = -(g\rho_a(h_s - h_{NL})(T_s - T_a)/T_s) + 1/2 C_{ps} \rho_a v_i^2$.

Here, C_{ps} is the wind pressure coefficient at the stack outlet. It is clear that d_p and h_{NL} are the two unknowns in Equations (9) and (10). Section 4.3 also identifies M_a as another unknown variable. Equations (6), (9) and (10) form 3 simultaneous nonlinear equations that can be used to solve for the problem of air flow through the heated stack that is subjected to the force of wind. The approach taken differs from those in Refs. [17,18]. Here, all phenomena are dealt with explicitly without any simplifying assumption and the equations are obtained from application of heat and mass balances.

4.5. Transmission of daylight through light pipe

Hien and Chirarattananon [21], use raytracing principle in calculating transmission of light rays through rectangular light pipes. The configuration of each flat section that together with other sections forms a rectangular light pipe is defined using plane geometry and each of its corner point is referenced to a Cartesian coordinate. When light rays traveling along a given direction incident on an internal surface, the rays are specularly reflected onto another surface. Daylight from the sun is considered to comprise collimated rays and raytracing method is used to trace its travel. However, for diffuse light from the sky, the method of flux transfer is used to calculate its transmission through a pipe. The authors in Ref. [21] encode the raytracing and flux transfer methods in a computer program called BESim. In this paper, the ASRC-CIE sky luminance model is used to model diffuse daylight, [25], and use raytracing to trace light rays from each of the standard 145 sky zones. The ASRC-CIE model uses four CIE sky models, clear, intermediate, overcast, and a high turbidity clear sky model. Perez's clearness index and brightness index in Ref. [25], calculated from values of measured beam irradiance and diffuse irradiance, are used to identify sky condition and to weigh contribution from each of the four CIE sky models. The model references zenith luminance.

5. Results and discussion

5.1. Ventilation

5.1.1. Design calculations for the ventilation stack

For ventilating the experimental room, the preliminary target was to have an air flow of $0.1 \text{ m}^3 \text{ s}^{-1}$, or about 10 air changes per hour in this experimental room. Assuming ventilation for 8 h per night and a rise in temperature of the air passing through the stack of $5 \text{ }^\circ\text{C}$, the amount of heat required on the air-side was about 4.0 kW h per day.

Average solar insolation per day at the location of experiment is 18.2 MJ m^{-2} or 5 kW h m^{-2} . Assuming an average efficiency of a solar collector of 50%, the required collector area is 1.6 m^2 . The collector available in the market, chosen and used in the experiments had an area of 2.16 m^2 and a water storage tank with a capacity 160 l.

The capacity of a small water pump available and used was 280 l per hour, or 0.078 l s^{-1} . The temperature drop of the hot water through the stack jacket was expected to be $1.5 \text{ }^\circ\text{C}$.

5.1.2. Experiments on ventilation

Experiments were conducted mainly during daytime to determine the amount of ventilation produced by the stack with solar heated water pumped through the water jacket. Measurements were made of the water flow rate, the temperature T_{wi} of the water entering the top of the stack, the temperature T_{wo} of the water from the bottom of the stack, the temperature T_s of the air emerging from the top of the stack and the air speed v_{in} into the bottom of the stack. Type K thermocouples were used for the temperature measurements, and hot wire anemometers were used for measuring the air speed into the stack. Measurements were also made of the wind speed and direction, the ambient air temperature T_a , and the ambient relative humidity outside the building.

The measured temperatures T_a , T_{wi} , T_{wo} , and T_s for an experiment conducted on a day in June 2010, when solar insolation was high and wind speed was low, are shown in Fig. 6. Fig. 7 shows the measured volumetric airflow rate \dot{V}_{sout} through the stack in the same experiment together with the calculated total airflow rate \dot{V}_{sin} . The distinctive patterns of the temperatures of the inlet T_{wi}

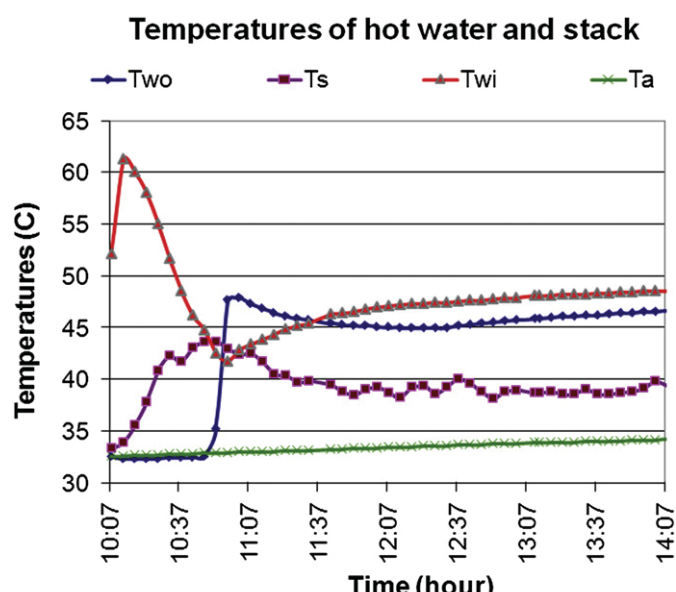


Fig. 6. Measured temperatures in the stack.

and that of the outlet T_{wo} hot water between 10.07 and 10.59 in Fig. 6 require a detailed examination. As is described subsequently, there are 3 distinct periods of the temperature patterns: 10.07 to 10.59, 10.59 to 12.00, and beyond 12.00.

Period 1: 10.07 to 10.59. At the start of the experiment, the water in the stack jacket was all at $32.5 \text{ }^\circ\text{C}$. The solar collector had accumulated hot water in its own tank during the previous day to stratify the water in the tank to different temperature levels. Fig. 8 together with Fig. 6 help illustrate the situation. Part of the water from the lowest stratification at the bottom of the tank, with temperature $45 \text{ }^\circ\text{C}$, had flowed by natural thermosyphon through the solar collector in the morning that resulted in raising the temperature of water in the top stratum to $62 \text{ }^\circ\text{C}$ when the pump operated to supply hot water to the jacket. Fig. 8a illustrates the situation at the start of the experiment at 10.07 h. Fig. 9 shows graphs of global solar irradiance, and of solar illuminance for the day, the two graphs at the top. The temperature of the water that flowed subsequently from the remainder of the solar

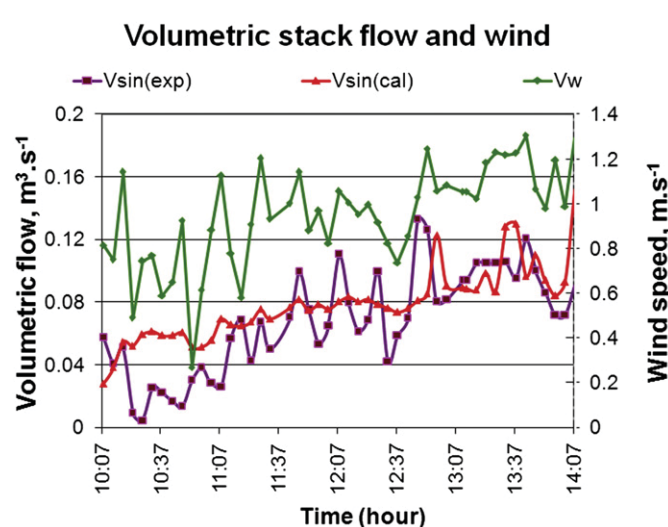


Fig. 7. Comparison between experimental and calculated volumetric airflow rates.

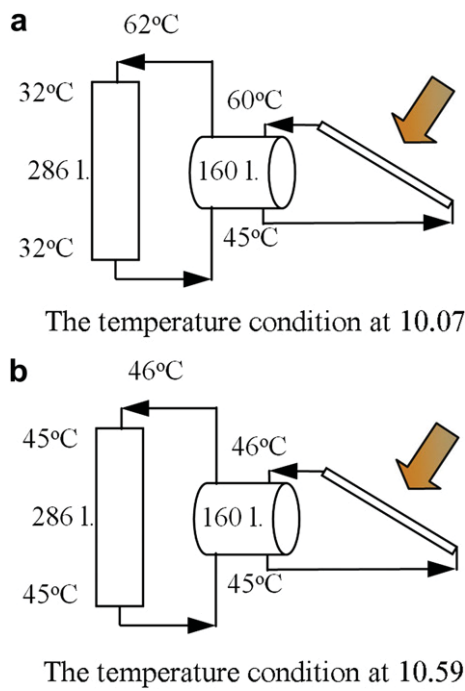


Fig. 8. Illustration of the water temperatures during the two periods.

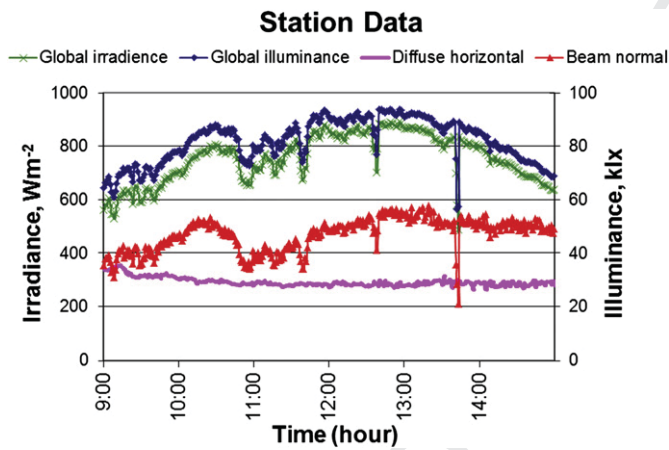


Fig. 9. Irradiance and illuminance on the day of experiment.

hot water tank into the stack jacket was lower while the temperature of the leaving water from the jacket, T_{wo} , remained at 32 °C. By 10.59 all water from the stack jacket had emptied into the solar collector tank and the mixture of water from the head of the jacket at 10.07, with temperature 48 °C, had reached the bottom of the jacket. During this period, heat from only the upper part of the jacket was transferred to air to drive the stack flow since the temperature of water at the lower part remained the same as that of the air in the stack. Effective height of the part of

the stack that drove air flow started from 0 m at the beginning to reach 3 m at the end of the period. Stack driven air flow was lowest during this period.

Period 2: 10.59 to 12.00. Fig. 8b illustrates the situation at the start of this period. The water in stack jacket had totally replaced the water in the solar water tank and this water had been heated by the solar collector to 45 °C. The temperature of the water in the jacket had reached 45 °C. Stack driven air flow had increased from the first period.

Period 3: from 12.00 onward. Solar radiation from a relatively clear sky had increased its intensity and the temperature at the top of the collector tank increased beyond 45 °C at the beginning of this period. The temperature of water flowing into the stack exceeded 48 °C near the end of the period. Stack driven air flow became highest in this period.

Summary of results. Table 2 shows average temperatures, wind speed, air flow, heat transfers and other quantities from the experiment for the 3 periods. The average inlet water temperature in Period 1 is higher than those of the other two periods. In period 2, the average outlet water temperature is higher than that at the inlet, thus straight forward calculation of heat transfer from hot water would give misleading results for Period 1 and 2. The values of log-mean temperature difference LMTD and heat transfer to air \dot{Q}_a in Period 3 are used in Equation (6) to obtain the air-side heat transfer parameter UA_a a value of 47.9 W K⁻¹. This value is used in the calculation of air flow through the stack to be described next.

5.1.3. Calculation of stack air flow

In applying Equations (1)–(10) for calculation of stack air flow, first the coefficients, exponents, and areas where air flows through of Equations (2)–(4) are set to values appropriate for the problem. Table 3 shows the given values, where the discharge coefficients, wind pressure coefficients and exponents assume values typically recommended [13–16]. Note that the wind was from the southwest direction. Next, the values of heat transfer parameters in Equations (7) and (8) are given as $M_w = 325.7 \text{ W K}^{-1}$ (for the pump flow of 280 l per minute) and $UA_a = 47.9 \text{ W K}^{-1}$.

In the experiment, the physical dimensions of the room and the stack are already known. From the experiment, the temperatures of entering water and of air into the stack are also known. In the absence of wind, there is no wind pressure at the openings into the room, and the air flows through the stack due to buoyancy force of the difference of air temperatures at the entry and exit of stack. The air temperature difference is due to heat transfer by water to air. In this case, the temperature of air at stack exit and the rate of air flow are two unknown variables in the heat transfer equation (6) or (7) and the stack flow equation (10). When wind exerts pressure at the openings it causes a counter balancing pressure d_p . This same pressure adds to the buoyancy pressure at the bottom of the stack. The number of unknowns becomes 3.

The problem of calculation of stack air flow now is reduced to the following problem statement: Given a set of values of condition of air at stack inlet (T_a and relative humidity), inlet water temperature, and wind velocity, find a set of values for v_a , stack air velocity, d_p , counter pressure to wind, h_{NL} , neutral height of air flow in the stack, that satisfy the flow balance and heat transfer equations (6),

Table 2
Experimental average temperature, air flow, and heat transfer values.

Period	Wind speed, m s ⁻¹	T_{wi} °C	T_{wo} °C	T_a °C	T_s °C	\dot{V}_{sin} m ³ s ⁻¹	\dot{Q}_a W	\dot{Q}_w W	LMTD	UA_a W K ⁻¹
1	0.71	51.9	32.6	32.8	39.8	0.025	152	NA	NA	NA
2	0.92	44.6	46.3	33.1	40.7	0.055	428	NA	7.67	NA
3	1.05	47.9	45.7	33.8	39.0	0.089	496	703	10.34	47.9

Table 3
Values of coefficients and exponents for Equations (2)–(4).

Air flow opening	North	East	South	West	Stack
Area (m ²)	0.1	0.1	0.1	0.1	0.237
Wind pressure coefficient	-0.231	-0.231	0.213	0.213	-0.297
Discharge coefficient	0.65	0.65	0.65	0.65	0.5
Exponent in (2) and (4)	0.65	0.65	0.65	0.65	0.65

(9) and (10). The solution to the three simultaneous nonlinear equations was obtained by the use of multiple-variable Newton Raphson numerical method. The first step in the calculation was to assume a value each for v_a , d_p , and h_{NL} . With given value of v_a , the heat capacity flow rate M_a and consequently the temperature T_a were calculated. These values were then used to calculate the left hand side functions in Equations (9) and (10). Numerical Jacobian (matrix of difference approximation to partial derivatives of functions) were then obtained and the calculation step continued.

In the experiment, all data were recorded on 1-min interval, but the measured input values were averaged as 5-min values for use in the calculation. The calculated volumetric stack air flow obtained is shown in the graph of Fig. 7, together with graphs of experimental values, and of wind speed.

For the first period, the effective stack height used in the calculation was varied linearly from 0 m at the beginning of the period to 3 m at the end of the period. The effective stack height for the other two periods was set at 3 m. The resulting graph of volumetric air flow appears to match reasonably well with that from experiment. However, since 5-min average values of inlet water temperature and wind speed were used in the calculation, the resulting graph appears smoother than that from experiment. The calculated volumetric flow rates of air through the stack for the 3 periods are obtained respectively as: 0.052, 0.071, and 0.093 m³ s⁻¹. These values are slightly larger than the corresponding values in Table 2. The corresponding RMSD (root of mean square difference between measured and calculated) values for each of the three periods and for the whole experiment are 0.034, 0.021, 0.056, and 0.027 m³ s⁻¹.

The fact that the method employed enable calculated results to match reasonable well with experimental results illustrates that this method of directly couple the three equations of wind pressure flow, stack pressure flow, and heat exchange through mass and heat balances is applicable. However, it is noted here that values of discharge coefficients are also highly relevant to the outcomes. The resultant volumetric air flow through the stack obtained corresponds to the value of discharge coefficient of 0.5 used.

5.2. Daylighting through light pipe

5.2.1. Experiment on the light pipe

During daytime the stack functions as a light pipe to transmit daylight into the building interior, as shown in Fig. 3. Measurements were made of the beam, diffuse and global illuminance using sensors in the daylight measurement station and the results are shown in Fig. 9. Measurements were also made of the total daylight illuminance at the top of the light pipe under the glass cover and the illuminance under the diffuser plate at the exit of the light pipe and the results are shown in Fig. 10. The very low illuminances before 10:20 and after 14:10 are caused by shading of the entrance to the light pipe by the slatted cover (see Fig. 4). At noon the illuminance at the entrance was 59 klux and the illuminance at the exit was 33 klux, giving a transmission of 56%, but at 12:40 the transmission was 84%. The sky of the day was relatively clear and beam illuminance featured prominently. The smaller angle between the beam rays and the pipe during noon led to the observed results. The

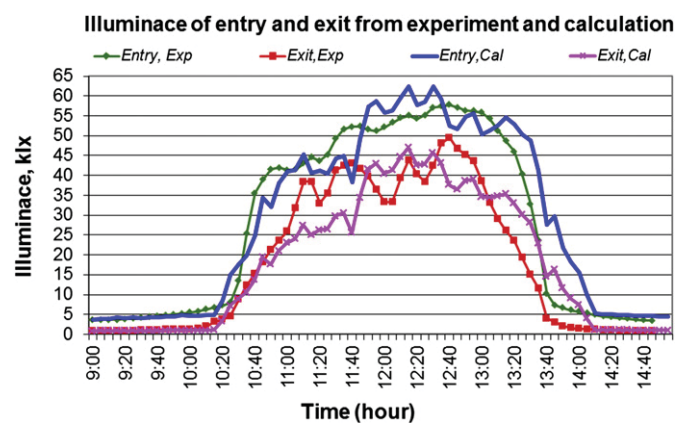


Fig. 10. Comparison between experimental and calculated daylight illuminances.

total flux of transmitted diffuse daylight was 2.5 kilo lumens (40 klux from Fig. 10 multiplied by 0.0635 m² of aperture area), which is about the same as the volume of light flux from a common long fluorescent lamp. This is sufficient for general illumination in the room.

5.2.2. Calculation of daylight transmission through the light pipe

The calculation of the daylight transmission through the light pipe was aided by the use of a modified version of BESim, where raytracing is now used for both daylight from sun and that from sky. There is fairly good agreement between the experimental and calculated values. The graphs in Fig. 10 include calculated daylight illuminance at light pipe entry to show that BESim could also handle shading from obstruction. The calculated results correspond to a light pipe transmission of 75%, similar to that from experiment.

6. Conclusion

The results from the experiment described in this paper demonstrate that a solar heated stack surrounding a light pipe can perform both function of providing cool natural ventilation air during night time and bringing daylight to the center of a large space in a house for general illumination during daytime. The specific configuration in this research differs from that described in Ref. [3] in that here there is a separate channel for ventilation air to flow, the light pipe itself is not used for air flow, and that hot water is used to transfer heat to air directly in the stack to create buoyancy force.

The results presented in this paper demonstrate that the simple method of calculation used is applicable. The significance of this result is that it is possible to utilize the method to design a system to achieve a rate of ventilation desired, to transmit given volume of light flux, and to evaluate the cost effectiveness of a configuration.

The specific experimental results illustrate that designed ventilation rate of 0.1 m³ s⁻¹ or 100 l s⁻¹ was achieved. However, it seems that the capacity of hot water tank used was not sufficient.

Acknowledgements

This work was jointly funded by the National Science and Technology Development Agency of the Ministry of Science and Technology and the National Research University Programme of the Commission for Higher Education of the Ministry of Education of Thailand.

References

- 1021
1022
1023
1024
1025
1026
1027
1028
1029
1030
1031
1032
1033
1034
1035
1036
1037
1038
1039
1040
1041
1042
1043
1044
1045
1046
1047
- [1] Economic and Social Statistic Bureau, National Statistical Office of Thailand, Statistics on household appliance ownerships. Available at: <<http://www.nso.go.th/keystat/keystatDB>>.
- [2] Z. Zhai, J.M. Previtali, Ancient vernacular architecture: characteristics categorization and energy performance evaluation, *Energy and Buildings* 42 (2010) 357–365.
- [3] K. Siren, T. Helenius, L. Shao, S. Smith, B. Ford, C. Diaz, A. Oliveira, S. Varga, J. Borth, E. Zaccheddu, Combining light pipe and stack ventilation, in: *World Renewable Energy Congress VI*, Brighton, 1–7 July 2000, pp. 395–400.
- [4] A.A. Elmualim, S. Smith, S.B. Riffat, L. Shao, Evaluation of dichroic material for enhancing light pipe/natural ventilation and daylighting in an integrated system, *Applied Energy* 62 (1999) 253–266.
- [5] G. Oakley, S.J. Smith, L. Shao, S.B. Riffat, TripleSave – the investigation and monitoring of a combined natural daylighting and stack ventilation system. CIBSE Conference Papers. Dublin, 2000.
- [6] L. Shao, S.B. Riffat, Daylighting using light pipes and its integration with solar heating and natural ventilation, *Lighting Research and Technology* 32 (2000) 133–139.
- [7] S. Varga, A.C. Oliveira, Ventilation terminals for use with light pipes in buildings: a CFD study, *Applied Thermal Engineering* 20 (2000) 1743–1752.
- [8] A.C. Oliveira, A.R. Silva, C.F. Afonso, S. Varga, *Applied Thermal Engineering* 21 (2001) 1925–1936.
- [9] K.S. Ong, A mathematical model of a solar chimney, *Renewable Energy* 28 (2003) 1047–1060.
- [10] K.S. Ong, C.C. Chow, Performance of a solar chimney, *Solar Energy* 74 (2003) 1–17.
- [11] D. Ryan, S.A.M. Burek, Experimental study of the influence of collector height on the steady state performance of a passive solar air heater, *Solar Energy* 84 (2010) 1676–1684.
- [12] K.T. Anderson, Theoretical considerations on natural ventilation by thermal buoyancy, *ASHRAE Transactions* 101 (2) (1995) 1103–1117.
- [13] D. Etheridge, M. Sandberg, *Building Ventilation: Theory and Measurement*, John Wiley and Son, Essex, 1996.
- [14] M.V. Swami, S. Chandra, Correlation for pressure distribution on buildings and calculation of natural ventilation air flow, *ASHRAE Transactions* 93 (1) (1987) 243–265.
- [15] M.V. Swami, S. Chandra, Procedure for Calculating Natural Ventilation Air Flow Rates in Buildings, final report FSEC-CR-163-86 (1987), Florida Solar Energy Center, Cape Canaveral, FL.
- [16] M.W. Liddament, *A Guide to Energy Efficient Ventilation*, AIVC, Coventry, UK, 1996.
- [17] M.H. Sherman, Superposition in infiltration modeling, *Indoor Air* 2 (1992) 101–114.
- [18] I.S. Walker, D.J. Wilson, Evaluating models for superposition of wind and stack effects in air infiltration, *Building and Environment* 28 (1993) 201–210.
- [19] H.F. Nouanegue, L.R. Alandji, E. Bilgen, Numerical study of solar-wind tower systems for ventilation of dwellings, *Renewable Energy* 33 (2008) 434–443.
- [20] B. Zamora, A.S. Kaiser, Numerical study on mixed buoyancy-wind driving induced flow in a solar chimney for building ventilation, *Renewable Energy* 35 (2010) 2080–2088.
- [21] V.D. Hien, S. Chirarattananon, An experimental study of a façade mounted light pipe, *Lighting Research and Technology* 41 (2009) 123–142.
- [22] S. Dutton, L. Shao, Raytracing simulation for predicting light pipe transmittance, *International Journal of Low Carbon Technologies* 2 (2008) 339–358.
- [23] P.D. Swift, R. Lawlor, G.B. Smith, A. Gentle, Rectangular-section mirror light pipes, *Solar Energy Materials and Solar Cells* 92 (2008) 969–975.
- [24] J.F. Kreider, P.S. Curtis, A. Rabl, *Heating and Cooling of Building: Design for Efficiency*, second ed. McGraw-Hill, Inc, Singapore, 2005.
- [25] R. Perez, P. Ineichen, R. Seals, J. Mechaels, R. Stewart, Modeling daylight availability and irradiance components from direct and global irradiance, *Solar Energy* 44 (1990) 271–289.
- 1048
1049
1050
1051
1052
1053
1054
1055
1056
1057
1058
1059
1060
1061
1062
1063
1064
1065
1066
1067
1068
1069
1070
1071
1072
1073
1074